VARIATIONS IN THE INTERPLANETARY MAGNETIC FIELD: MARINER 2

Part 2. Interpretation in Terms of Hydromagnetic Waves

Paul J. Coleman, Jr.

Publication Number 504

Institute of Geophysics and Planetary Physics
University of California, Los Angeles
Los Angeles 24, California

Preprint
May 5, 1966

Abstract

Some characteristics of the variations of the interplanetary magnetic field and the plasma velocity, observed during the flight of Mariner 2, are considered. First, properties of the power spectra from records of the plasma velocity and the three vector components of the field are described. Next, the properties of the cross spectra between pairs of this set of four variables are described. The variations that would be produced in the plasma velocity and the field components by hydromagnetic waves are determined from a model of a uniform, perfectly conducting, isentropic, ideal gas in a uniform magnetic field. The properties of the variations determined empirically, are compared with those determined from this model. The following conditions, found to be necessary in the model, are found to be satisified by the observed variations:

(1) Significant coherences were usually present between all pairs of measured variables.

(2) The phase differences between each pair were independent of frequency.

(3) The ratios of the power densities for each pair were independent of frequency.

(4) The values of these ratios fall in the ranges established from the model.

(5) The values of the phase differences were either 0° or 180°.

(6) The phase differences changed by 180° when the direction of the interplanetary field changed from inward toward the sun to outward.

VARIATIONS IN THE INTERPLANETARY MAGNETIC FIELD: MARINER 2

Part 2. Interpretation in Terms of Hydromagnetic Waves

Paul J. Coleman, Jr.
Institute of Geophysics and Planetary Physics
University of California, Los Angeles
Los Angeles 24, California

The properties of the ionized gases and magnetic fields observed in interplanetary space suggest that the medium would support the propagation of hydromagnetic waves through this region [c.f. Alfvén, 1950]. In Part 1 [Coleman, 1966], some properties of the variations in the magnetic field and plasma velocity, observed during the flight of Mariner 2, were described. In this second part, these properties will be compared to the properties of variations that would be produced by hydromagnetic waves in a highly idealized case. The primary purpose of this paper is to show that most of the properties of the variations in the magnetic field and plasma velocity satisfy certain necessary conditions of hydromagnetic wave behavior.

The data to be discussed here were obtained with the magnetometer and ion spectrometer, or plasma probe, on board Mariner 2, which was launched in August, 1962. Measurements of three orthogonal vector components of the field and of the velocity of the interplanetary plasma were obtained during the four-month flight of Mariner 2 between the earth and Venus.

It will be convenient to employ heliocentric, spherical, polar coordinates with the polar axis coincident with the sun's axis of rotation. Thus, the positive r direction is radially outward from the sun, the ϕ direction is parallel to the solar equatorial plane and positive in the direction of planetary motion, and the θ direction completes the usual right-handed system. In this system, the quantities measured with the magnetometer and plasma probe on board Mariner 2 are the three vector components of the magnetic field, B_r, B_θ, and B_ϕ, and the plasma velocity $V = V_r$. Unit vectors in the r, θ, and ϕ directions at the position the spacecraft,(r, θ, ϕ), are shown in Figure 1.

Estimates of the auto spectra and cross spectra from records of the four measured variables have provided the empirical results which are to be discussed here. In the next section, we will describe a model for hydromagnetic disturbances. We will then compare the observations and the model.

The Model

We wish to compare the observed variations in the plasma velocity and the magnetic field with the variations that would be produced by hydromagnetic waves in the interplanetary plasma. Following Thompson, [1962], with minor changes in notation, we will consider plane-wave perturbations in the plasma displacement, $\vec{d}$, moving through a uniform, perfectly conducting, isentropic, ideal gas in a uniform magnetic field $\vec{B}_o$ for the case in which the gas is moving with a bulk velocity $\vec{V}_o$. For such a system, in the reference frame moving with velocity $\vec{V}_o$, the linearized equations are

$$\partial\rho/\partial t + \rho_o \nabla \cdot \vec{v} = 0 \qquad (1)$$

$$\rho_o(\partial\vec{v}/\partial t) = -\nabla p + (1/4\pi)\ (\nabla \times \vec{b}) \times \vec{B}_o \qquad (2)$$

$$\partial p/\partial t - (\gamma p_o/\rho_o)\ (\partial\rho/\partial t) = 0 \qquad (3)$$

$$\vec{E} + (\vec{v}/c) \times \vec{B}_o = 0 \qquad (4)$$

$$(1/c)\ \partial\vec{b}/\partial t = -\nabla \times \vec{E} \qquad (5)$$

where ρ_o is the mean density and ρ is the density perturbation, $\vec{V} = \vec{V}_o + \vec{v}$ is the velocity, $\vec{B} = \vec{B}_o + \vec{b}$ is the magnetic field, p_o is the mean pressure and p is the pressure perturbation, $\vec{E}$ is the electric field, γ is the ratio of specific heats for the plasma, and c is the velocity of light. It has been assumed that $\vec{V}_o$ and $\vec{B}_o$ are constant and uniform.

Initially we will employ rectangular coordinates x y z. Since the magnetic field $\vec{B}_o$ is uniform, we assume $\vec{B}_o = B_o\hat{x}$ where $\hat{x}$ is a unit vector in the positive x direction. Since the system is symmetrical about the x axis, it will also be convenient to describe the orientation of an arbitrary vector $\vec{a}$ in terms of the angles θ_a and ϕ_a. Here $\theta_a = \cos^{-1}(\vec{a} \cdot \hat{x}/a)$ and $\phi_a = \cos^{-1}(\vec{a}_\perp \cdot \hat{y}/a_\perp)$ where $\vec{a}_\perp$ is the projection of $\vec{a}$ on the yz plane. Thus, $a_y = a_\perp \cos \phi_a$ and $a_z = a_\perp \sin \phi_a$ and $a_\perp = a \sin \theta_a$. These quantities are depicted in Figure 2.

From Equations 4 and 5, to the first order in $\vec{b}$ and $\vec{v}$,

$$\begin{aligned} \partial\vec{b}/\partial t &= \nabla \times (\vec{V} \times \vec{B}) \\ &= \nabla \times (\vec{v} \times \vec{B}_o) \end{aligned} \tag{6}$$

Assuming that the displacement $\vec{d}$ and the velocity $\vec{v}$ are small so that in this linear approximation $\partial\vec{d}/\partial t = \vec{v}$, integration of Equation 6 yields

$$\vec{b} = \nabla \times (\vec{d} \times \vec{B}_o) \tag{7}$$

This expression fixes the relationship between the vector components of $\vec{b}$ and $\vec{d}$ transverse to $\vec{B}_o$. For a plane wave in the displacement, it also fixes the relationship between $\vec{b}$ and $\vec{v}$. Thus, digressing briefly, we may consider the plane wave with propagation velocity $U\hat{k}$ relative to a system moving with velocity $\vec{V}_o$, the streaming velocity of the plasma. In this case,

$$\vec{d} = \vec{d}_o \exp\{(2\pi i/\lambda)[\vec{k} \cdot (\vec{r} - \vec{V}_o t) - Ut]\} \tag{8}$$

Note that $\hat{k}$ is a unit vector in the direction of propagation. In the frame of reference moving with the plasma,

$$\vec{d} = \vec{d}_o \exp [(2\pi i/\lambda) (\vec{k} \cdot \vec{r} - Ut)] \tag{8a}$$

and

$$\vec{v} = \partial\vec{d}/\partial t = (-2\pi i/\lambda) U\vec{d} \tag{9}$$

Also

$$\partial\vec{d}/\partial x = (2\pi i/\lambda) k_x \vec{d} = (-k_x/U) \vec{v}$$

$$\partial\vec{d}/\partial y = (-k_y/U) \vec{v} \tag{10}$$

$$\partial\vec{d}/\partial z = (-k_z/U) \vec{v}$$

Then, from Equation 7 and Equations 10,

$$\vec{b} = \vec{b}_o \exp [(2\pi i/\lambda) (\vec{k} \cdot \vec{r} - Ut)]$$

$$\vec{b} = (B_o/U) [\hat{x}(k_y v_y + k_z v_z) + \hat{y} (-k_x v_y) + \hat{z} (-k_x v_z)] \tag{11}$$

$$= (B_o/U) [\hat{x} (\vec{k}_\perp \cdot \vec{v}_\perp) + \hat{y} (-k_x v_\perp \cos \phi_v) + \hat{z} (-k_x v_\perp \sin \phi_v)]$$

This relationship is based only upon the assumption that the plasma is highly conducting, i.e., it is based upon Equations 4 and 5. The additional requirement that Equations 1 - 3 be satisifed, determines

the remaining properties of the plane waves which may propagate through such a plasma.

Returning now to Thompson's development, if $\vec{d} = 0$ at the time $t = 0$, integration of Equation 1 yields

$$\rho + \rho_o \nabla \cdot \vec{d} = 0 \tag{12}$$

Integration of Equation 3 and substitution for ρ from Equation 12 yields

$$p = -\gamma p_o \nabla \cdot \vec{d} \tag{13}$$

Combining Equations 2 and 13, we obtain

$$(\partial^2 \vec{d}/\partial t^2) - (\gamma p_o/\rho_o) \nabla (\nabla \cdot \vec{d}) - (1/4\pi) (\nabla \times \vec{b}) \times \vec{B}_o = 0 \tag{14}$$

Next, we denote the Alfvén speed by $C_A = B_o/(4\pi\rho_o)^{1/2}$, the sound speed by $C_S = (\gamma p_o/\rho_o)^{1/2} = (\gamma kT)^{1/2}$, and a unit vector in the direction of $\vec{B}_o$ by $\hat{e}$. Equation 14 may then be written

$$(1/C_A^2) (\partial^2 \vec{d}/\partial t^2) - [(C_S^2 + C_A^2)/C_A^2] \nabla (\nabla \cdot \vec{d})$$

$$+ \nabla (\hat{e} \cdot \nabla) (\hat{e} \cdot \hat{d}) - (\hat{e} \cdot \nabla)^2 \hat{d} + (\hat{e} \cdot \nabla) (\nabla \cdot \vec{d}) \hat{e} = 0 \tag{15}$$

If we consider plane wave solutions of the form given by

Equation 8a, the vector components of Equation 15 become

$$(U^2/C_A^2)\, d_i + A_{ij} d_j = 0 \tag{16}$$

where the A_{ij} are functions of $\hat{e}$, $\hat{k}$, and C_S^2/C_A^2, and i, j = x, y, z.

The physical significance of this set of equations is more readily seen if we consider the independent variables $\hat{k} \cdot \hat{d}$, $\hat{e} \cdot \hat{d}$, and $\hat{e} \cdot \hat{k} \times \vec{d}$ rather than the vector components d_i of $\vec{d}$. Then Equations 16 yield

$$[(U^2 - C_A^2 - C_S^2)/C_A^2]\, \hat{k} \cdot \vec{d} + (\hat{e} \cdot \hat{k})\, (\hat{e} \cdot \vec{d}) = 0 \tag{17}$$

$$(U^2/C_A^2)\, \hat{e} \cdot \vec{d} - (C_S^2/C_A^2)\, (\hat{e} \cdot \hat{k})\, (\hat{k} \cdot \vec{d}) = 0 \tag{18}$$

$$[(U^2/C_A^2) - (\hat{e} \cdot \hat{k})^2]\, \hat{e} \cdot \hat{k} \times \vec{d} = 0 \tag{19}$$

From these equations, we see that one root is the velocity of an Alfvén wave $U_A^2 = C_A^2 \cos^2 \theta_k$ where $\hat{e} \cdot \hat{k} = \cos \theta_k$. The other two roots are the roots of the quadratic

$$(1/C_A^4)\, U^4 - [(C_A^2 + C_S^2)/C_A^2]\, U^2 + (C_S^2/C_A^2) \cos^2 \theta_k = 0 \tag{20}$$

or

$$U_{\pm} = (1/\sqrt{2}) \left\{(C_A^2 + C_S^2) \pm [(C_A^2 + C_S^2)^2 - 4C_S^2 C_A^2 \cos^2 \theta_k]^{1/2}\right\}^{1/2} \quad (21)$$

where the wave with velocity U_+ is designated the 'fast' wave and the wave with the velocity U_- is designated the 'slow' wave.

From Equation 19, we see that the vectors $\vec{d}$, $\hat{k}$, and $\vec{B}_o = B_o \hat{e}$ are co-planar. From Equation 17, we see that

$$(\vec{k}_\perp \cdot \vec{d}_\perp)_\pm = - [(U_\pm^2 - C_S^2)/(U_\pm^2 - C_A^2 - C_S^2)] \, k_\parallel d_\parallel \quad (22)$$

$$= A_\pm k_\parallel d_\parallel$$

where the subscripts $\perp$ and $\parallel$ are used respectively to designate components transverse and parallel to $\vec{B}_o$. This expression must be satisfied by both fast and slow waves. Note that A_+ is positive and A_- is negative.

Since measurements of $\vec{v} = \partial \vec{d}/\partial t$ and $\vec{b}$ are available, we must consider the behavior of $\vec{v}$. Since $\vec{v}$ is 90° out of phase with $\vec{d}$, we have

$$\vec{v} = \vec{v}_o \exp (2\pi i/\lambda) \, [\hat{k} \cdot \vec{r} - Ut - \lambda/4] \quad (23)$$

with $\vec{v}_o$ parallel to $\vec{d}_o$.

Since $\hat{k}$ and $\vec{B}_o$ are constant, the geometrical relationships between $\vec{d}_o$, $\hat{k}$, and $\vec{B}_o$ hold also for $\vec{v}_o$, $\hat{k}$, and $\vec{B}_o$. Now from the results obtained thus far, we can obtain $\vec{v}_o$ in terms of v_o, θ_k, ϕ_k, C_A, and C_S, i.e., we can determine the direction of $\vec{v}_o$. Then, from Equation 11,

we can compute $\vec{b}_o$.

For Alfvén waves, $v_x = 0$ and $\vec{v}_o$ is transverse to both $\vec{B}_o$ and $\hat{k}$. Thus, if $\hat{k}$ is parallel to $\vec{B}_o$, $\vec{v}_o$ may have any direction transverse to $\vec{B}_o$. If $\vec{k}_\perp \neq 0$, $\vec{v}_o$ must be transverse to both $\vec{B}_o$ and $\hat{k}$. We may arbitrarily select the phase of $\vec{v}$ so that $\vec{v}_o$ is parallel to $\vec{B}_o \times \hat{k}$. Then $\phi_v = \phi_k + \pi/2$. Thus, for an Alfvén wave

$$v_x = 0$$

$$v_y = v \cos (\phi_k + \pi/2) \tag{24}$$

$$v_z = v \sin (\phi_k + \pi/2)$$

For fast and slow waves,

$$v_x = v \cos \theta_v$$

$$v_y = v \sin \theta_v \cos \phi_v \tag{25}$$

$$v_z = v \sin \theta_v \sin \phi_v$$

so from Equation 22,

$$k_\perp v_\perp (\cos \phi_k \cos \phi_v + \sin \phi_k \sin \phi_v)_\pm = A_\pm v_x k_x \tag{26}$$

Now $\vec{B}_o$, $\hat{k}$, and $\vec{v}_o$ are co-

planar for fast and slow waves, so that $\phi_v = \phi_k$ or $\phi_k + \pi$. Thus, the coefficient of $k_\perp v_\perp$ is ± 1. But A_+ is positive and A_- is negative, so for fast waves $\phi_v = \phi_k$, while for slow waves $\phi_v = \phi_k + \pi$.

Then from Equation 25,

$$(v_\perp / v_x)_\pm = |A_\pm| \; (k_x / k_\perp)$$

or

$$(\tan \theta_v)_\pm = |A_\pm| \cot \theta_k \tag{27}$$

These results may be summarized by the following relations:

Alfvén Waves

$$b_x = 0$$

$$b_y = -v(B_o/U_A) \cos \theta_k \cos (\phi_k + \pi/2) \tag{28}$$

$$b_z = -v \; (B_o/U_A) \cos \theta_k \sin (\phi_k + \pi/2)$$

Fast and Slow Waves

$$b_x = \pm v(B_o/U_\pm) \sin \theta_k \sin \theta_v$$

$$b_y = \mp v(B_o/U_\pm) \cos \theta_k \cos \phi_k \sin \theta_v \qquad (29)$$

$$b_z = \mp v(B_o/U_\pm) \cos \theta_k \sin \phi_k \sin \theta_v$$

where the upper signs correspond to fast waves, the lower signs correspond to slow waves, and θ_v is given by Equation 27.

From this model, for each of the three modes, given $\vec{B}_o$, the direction of propagation defined by θ_k and ϕ_k, the number density of the protons, the temperature, and the magnitude of the velocity perturbation v_o, one may calculate $\vec{b}_o$ and the orientation of $\vec{v}_o$.

During the flight, the average value of B_o was about $5\gamma = 5 \cdot 10^{-5}$ gauss. The average number density of the protons, n_p, near 1 AU was about 5 cm^{-3}, and the average proton temperature was $1.7 \cdot 10^5$°K. [Neugebauer and Snyder; 1963, 1966]. Thus, $C_A \approx 5 \cdot 10^6$ cm/sec and $C_S \approx 4 \cdot 10^6$ cm/sec. From Equation 10 and the properties of the different types of waves, we can determine the amplitudes of the components of $\vec{v}$ and $\vec{b}$ in terms of the amplitude v_o. The quantities v_x, $v_\perp$, b_x, and $b_\perp$ are listed in Table 1 for each of the three modes and for θ_k = 0, 15, 30, 45, 60, 75, and 90°.

The quantities that were measured are B_r, B_θ, B_ϕ, and $V = |\vec{V}|$. Since the average radial streaming velocity of the plasma was so much greater than the average value of the velocity perturbation as determined from the auto spectra of V, we may assume $V \approx V_r$.

In order to compare the greatly idealized model with the observations, it is necessary to assume that the average interplanetary field,

as well as the plasma temperature and density are piecewise uniform. Then we may establish the vector components of $\vec{v}$ and $\vec{b}$ in the $r\theta\phi$ system, given Equations 27 and 28 and the orientation of $\vec{B}_o = \hat{r}\, B_{or} + \hat{\theta}\, B_{o\theta} + \hat{\phi}\, B_{o\phi}$.

Suppose $\alpha = \tan^{-1}(-B_{o\phi}/B_{or})$ and $\beta = \tan^{-1}(B_{o\theta}/B_L)$, where $B_L = (B_{or}^2 + B_{o\phi}^2)^{1/2}$. These angles are shown in Figure 1. Then from the geometry of the system, for $i = r, \theta, \phi$,

$$v_i = \sum_j a_{ij}\, v_j \tag{30}$$

and

$$b_i = \sum_j a_{ij}\, b_j \tag{31}$$

where $j = x, y, z$, the v_j's are given by Equations 24 or 25, and the b_i's are given by Equations 28 and 29, and

$$a_{ij} = \begin{vmatrix} \cos\beta\cos\alpha & -\sin\beta\cos\alpha & \sin\alpha \\ \sin\beta & \cos\beta & 0 \\ -\cos\beta\sin\alpha & \sin\beta\sin\alpha & \cos\alpha \end{vmatrix} \tag{32}$$

Our analysis of the Mariner-2 data provides estimates of the auto spectra of the measured variables V_r, B_r, B_θ, and B_ϕ and estimates of the cross spectra of all the possible pairs of these variables. From Equations 14 and 15 in terms of the scalar amplitude v_o, we may determine the power P that would appear in the records of V_r, B_r, B_θ, and

B_ϕ as a result of these idealized waves. We may also determine the coherences and phase relations among these variables in the idealized case. The power that would appear in the record of a measured variable, due to a single idealized wave, is just the average value of the square of the variable. Thus, $P(v_r) = \langle v_r^2 \rangle$ and $P(b_i) = \langle b_i^2 \rangle$, $i = r, \theta, \phi$. Since the terms $a_{ij} v_j$ and $a_{ij} b_j$ are all related by real multiplicative factors, the cross spectra of the variables will yield real values. Thus, the values of the squares of the coherences, R, and phase differences for each pair of variables may be obtained from the expressions

$$R = \langle v_i \, b_j \rangle / \langle v_i^2 \rangle \langle b_j^2 \rangle \qquad \text{for any } i, j$$

$$R = \langle b_i \, b_j \rangle / \langle b_i^2 \rangle \langle b_j^2 \rangle \qquad \text{for } i = j$$

where $k, j = r, \theta, \phi$. Here $|R|$ is equivalent to the coherence squared and the sign of R determines whether the variables are in phase (+) or 180° out of phase (-).

During the flight, the preferred value of the angle α was about 40°. During periods in which the field was directed predominantly outward from the sun, the preferred value of B_θ was about 1.9γ. Thus, the preferred value of β was typically about 22°. However, the measurements of the absolute value of B_θ are less reliable than those of B_r and B_ϕ. As a result, values of P and R were computed for the cases $\beta = 0$ and 25° in order to establish the effects of errors in the

estimates of β. Further, there is evidence, the reliability of which is similarly questionable because of the uncertainty in the absolute values of B_θ, that the average value of B_θ remained positive during the periods in which the interplanetary field was directed back toward the sun. This is the case in which $\alpha = 40 + 180°$, $\beta = 25°$, which is simply related to the case in which $\alpha = 40°$, $\beta = -25°$. As a result, the latter case was also considered.

It has been assumed that the waves are circularly polarized. Since $\vec{B}$, $\vec{k}$, and $\vec{v}$ are co-planar for fast and slow waves, the angle ϕ_k will be used to indicate the orientation of the plane of polarization of such a wave. There is no reason a priori for the waves to have a preferred plane of polarization in a uniform system. In this case, the values of ϕ_k would be determined by the properties of the source of the disturbances. In interplanetary space, non-uniformity of $\vec{B}_o$, $\vec{V}_o$, ρ_o, and p_o, may lead to asymmetries in the system which in turn may constrain ϕ_k to certain allowed values. However, since we were approximating the actual system by a uniform one, we considered first the case in which the disturbances are produced by the superposition of a great many plane waves with random phases and with the orientations of the planes of polarization distributed uniformly. In other words, we considered the case of circularly polarized waves. Thus, in taking the average value of the squares of the variables and of the products of the different variables, we assumed that, when averaged over all the present waves,

$$\langle f_1(t)\, f_2(t) \sin \phi_k \cos \phi_k \rangle = 0$$

$$\langle f_1(t)\, f_2(t) \sin \phi_k \rangle = \langle f_1(t)\, f_2(t) \cos \phi_k \rangle = 0$$

i.e., we assumed no coherence on the average between v_i and v_j, or b_i and b_j, or v_i and b_j, $i \neq j$, k, $j = x, y, z$.

Under these assumptions, the values of $P(v_r)$, and $P(b_i)$, for $i = r, \theta, \phi$, and the values of $R(v_r, b_i)$, for $i = r, \theta, \phi$, and $R(b_i, b_j)$, for $i \neq j$, and for $i, j = r, \theta, \phi$, may be computed in terms of v_o for any field orientation and propagation direction. These values are, of course, independent of the frequency f of the waves. This frequency, measured in the frame of reference moving with the plasma, is $f = U/\lambda$.

If we assume that all the waves originate within a finite region of space centered at the sun, on the average, disturbances produced by waves propagating outward from the sun will predominate. However, since a point source in a uniform field will produce a spherically spreading disturbance in the fast mode and disturbances moving along the field lines in both directions in the transverse and slow modes, we assume that waves moving back toward the sun also contribute to the observed variations in $\vec{v}$ and $\vec{b}$. The phase relationships between $\vec{b}$ and $\vec{v}$ for a wave moving in the $\vec{k}$ direction, back toward the sun, differs by 180° from that for a wave moving outward. Thus, any contribution to $\vec{b}$ from inwardly traveling waves will reduce the coherences indicated by $|R|$, between v_r and b_i, $i = r, \theta, \phi$, but will not change

the phase relationships so long as the contribution from outwardly traveling waves predominates. Accordingly, the calculated values of R are those for the outwardly traveling waves, or $k_x = \cos \theta_k \geq 0$. The various cases for which P and R have been computed may be summarized as follows:

Modes:	Alfvén, Fast, Slow
θ_k:	0, 15, 30, 45, 60, 75, 90°
β:	±25, 0°
α:	40°
Polarization:	Circular
B_o:	5.0γ
ρ_o:	5 m_p gm cm^{-3} (m_p = 1 proton mass)
T:	10^5°K

The results are listed in Table 1.

For our purposes the most significant parameters listed in the table are the ratios $P(b_i)/P(v_r)$, i = r, θ, φ, since these quantities are directly measurable from the power spectra of V_r and B_i, i = r, θ, φ. Note that they are also independent of the signs of B_o and k_x. Another important aspect of these results is the indication that v_r and b_r are 180° out of phase regardless of which type of wave is considered, except for fast waves when $\theta_k > 75°$. For the transverse and slow waves this result is apparent from an inspection of Equations 14 and 15, respectively. Of course, all the listed phase relationships are changed

by 180° when B_o is negative.

In considering the phase relationships, we have focused our attention on the variables v_r and b_r because the equations indicate that the phase relationship and the coherence are the least dependent upon the sign and magnitude of β in this case.

Observations

As mentioned previously, the variables measured by the magnetometer and plasma probe are B_r, B_θ, B_ϕ, and V_r. In the analysis of the data, discussed in Part 1, amplitude distributions of these variables were examined. It was found that the distributions were roughly Gaussian.

Next, the records were examined for correlations between the various pairs of these variables. The procedure employed was the usual one of obtaining estimates of the cross spectra of each pair of variables for several sections of the record. It was found that each pair of variables exhibited significant coherence on the average, and that the coherence was particularly strong for the pair V_r, B_r. Further, the phase differences were usually found to be either 0° or 180° and roughly independent of frequency. These results from the cross spectra provided strong evidence for wave-like motions in the interplanetary plasma, and led to the somewhat more quantitative comparison, the results of which will be summarized next.

We will be concerned with data obtained during four 10-day periods and two 6-day periods indicated in Table 2. These periods were selected in order to exclude the major reversals of the polarity of the interplanetary field, i.e., changes of the algebraic sign of B_o, that occurred twice during each period of solar rotation [Coleman, Davis, Smith, and Jones, 1966]. These changes were also discussed in Part 1. Thus, during each of these periods, the polarity of the field was nearly always that listed in Table 2.

We will consider the frequency range from 1 to 50 cycles per day (cpd).

The lower limit was selected in order to limit the computer time required for the analysis. An upper limit of 100 cpd was imposed by the sampling rate of the plasma probe. Indications of significant aliasing between 50 and 100 cpd in some of the power spectra of V_r prompted the selection of 50 cpd as the upper limit.

In the frequency range 1 - 50 cpd, then, the auto spectra of B_r, B_θ, B_ϕ, and V_r provided estimates of the power densities for these variables as functions of the frequency. As the first step in the comparison between the measured properties of the variations in B_r, B_θ, B_ϕ, and V_r and the properties of b_r, b_θ, b_ϕ, and v_r determined from the model of idealized hydromagnetic waves, various ratios of the spectral densities were computed as functions of the frequency, f, for the six sets of data. The ratios $P(B_r)/P(V_r)$, $P(B_\theta)/P(V_r)$, and $P(B_\phi)/P(V_r)$ are plotted versus f in Figure 3.

In the ideal case, considered in the last section, these ratios are independent of frequency, at least for cases in which the frequencies of the waves, measured in the reference frame moving with the streaming velocity of the plasma, are smaller than the proton gyro frequency which is about 0.08 cps in a field of strength 5γ. In the empirical cases, the power-density ratios are evidently independent of frequency, since the ratios plotted in Figure 3 show no apparent frequency dependence.

In the ideal case, the values of these power density ratios for a particular plane wave depend upon the geometry of the system and upon the field magnitude, $\vec{B}_o$, the temperature, T, and density, ρ_o, of the

gas. For Alfvén waves, the values are independent of $|\vec{B}_o|$. The values computed for the ideal case, as described in the preceding section, are also indicated on the right-hand side of Figure 3. In the empirical cases, the values of the power-density ratios were generally within or close to the ranges determined for the ideal case. The variations among the empirical cases are probably due primarily to variations in $|\vec{B}_o|$, ρ_o, and T.

Comparison of the measured values and the theoretical values of the power-density ratios also indicates that waves in the transverse and/or fast modes were present, since the measured ratios are considerably greater than the ratios expected for slow waves, except for θ_k near 90°, but are generally within the ranges of the ratios expected for the other two modes. This result does not imply that slow waves were absent but rather that Alfvén and/or fast waves were present and, therefore, contributed most to the variations in the field. Evidence that the observed field variations could not be produced by purely transverse waves was presented in Part 1, in which it was shown that the variations in B_w, the magnitude of the vector component of the field in the direction of the ideal spiral field, were of roughly the same magnitude as the variations in the other vector components.

However, to this point, the most significant results of this comparison are simply that the measured values of the power-density ratios are evidently independent of frequency and that these values are

in the ranges calculated for the idealized waves using only the measured values of the mean proton density, the mean field strength, and the mean proton temperature.

Having considered the properties of the auto spectra of the measured variables B_r, B_θ, B_ϕ, and V_r, let us turn to the cross spectra of various pairs of these variables. The cross spectra of a pair of variables provides estimates of $|R|$, the magnitude of the square of the coherence between the two time series corresponding to the two variables, as a function of frequency, and estimates of Φ, the difference in the phase of the predominant coherent components of the two variables, as a function of frequency.

In effecting the comparison between the empirical cases and the ideal case, the quantities $|R|$ and Φ, calculated for pairs of the measured variables were compared, respectively, with $|R|$ and the algebraic sign of R calculated for the corresponding pair of variables for the ideal case, as described in the preceding section. Thus, for the ideal case, if $R > 0$, $\Phi = 0°$. If $R < 0$, $\Phi = 180°$. Also, for the ideal case, R is independent of frequency.

Cross spectra were computed for all pairs of the measured variables for all six periods of interest. The values of $|R(V_r, B_r)|$, the square of the coherence for the pair of variables V_r and B_r, was greater by factors in the range from 5 to 8 than the values of $|R|$ for any of the other pairs, although on the average, all pairs exhibited significant coherences. Accordingly, only values of

$|R(V_r, B_r)|$ and $\Phi(V_r, B_r)$ are reproduced in Table 2. Values for all pairs are given in Part 1.

In most cases, the quantity $|R(V_r, B_r)|$ exhibited considerable frequency dependence over the range 1 - 100 cpd, as shown in Figure 21 of Part 1. However, in the frequency range 1 - 50 cpd, the average value is sufficient for our purposes. Furthermore, the quantity $\Phi(V_r, B_r)$ is roughly independent of frequency. Thus, only average values of $|R|$ and Φ, taken over the frequency range 1 - 50 cpd, are listed in Table 2.

From Table 2, it is apparent that the coherence of V_r and B_r was relatively high and that these two variables were nearly 180° out of phase when the average field was directed from the sun (+ polarity) and nearly in phase when the average field was directed toward the sun (- polarity). The method by which this polarity was reckoned is described in Part 1. The apparent differences in Φ of -10° to -15° from 0° to 180° is a phase effor resulting from the manner in which the time was assigned to the measurements of V_r, rather than the result of any real phase differences.

Phase differences of 180° and 0° for positive and negative polarities, respectively, are consistent with the results of the computations in the preceding section for the ideal case in which the waves propagate primarily outward, i.e., propagate with $k_x \geq 0$. As mentioned previously, we might expect the coherences to be well below the values for the ideal waves because of the effects of waves propagating back toward the sun, i.e., propagating with $k_x < 0$.

Summary

In the foregoing, various properties of simultaneous variations observed in the interplanetary magnetic field and in the velocity of the solar-wind plasma were compared to the properties of hydromagnetic waves as determined from an idealized model.

The qualitative study of the observed variations yielded the following results over the frequency range, 1 - 50 cpd:

(1) Significant coherences were usually exhibited between all pairs of the set of variables B_r, B_θ, B_ϕ, and V_r.

(2) The coherences generally varied with frequency. For the cases in which the values were consistently significant, the coherences decreased with increasing frequency.

(3) The phase differences of the predominant coherent components in each pair of variables were roughly independent of frequency.

(4) The ratios of the power densities for each pair of variables were similarly independent of frequency.

Comparison with the properties of the idealized waves showed that the first, third, and fourth properties listed above would be expected for any complex group of waves as long as the amplitudes of the waves in one mode relative to the amplitudes of the waves in each of the other two modes are roughly the same at any of the frequencies studied. The second property listed above would be expected if, for example, the waves that were encountered were to include two such

groups of waves, each with a different power spectrum and a different phase relationship.

The quantitative study of the observed variations yielded the following results:

(5) Most of the measured values of the power-density ratios, $P(B_i)/P(V_r)$, $i = r, \theta, \phi$, were in the ranges of the values that were calculated for the ideal waves. The measured values were generally close to the maxima of these calculated ranges.

(6) The measured values of the power-density ratios, given in Table 2, show that $P(B_\theta)/P(V_r) > P(B_\phi)/P(V_r) > P(B_r)/P(V_r)$. The results calculated for the ideal waves, listed in Table 1, show that this relationship would be expected for all Alfvén waves and for fast waves with $\theta_k < 45°$.

(7) The phase differences of V_p and B_r, as measured by their cross spectra, were either 0° or 180°. The value of 0° was observed when the spiral interplanetary field was directed toward the sun. The value of 180° was observed when the field was directed away from the sun.

(8) The measured values of the coherences, listed in Table 2, were found to be considerably smaller than the values calculated for the ideal waves and listed in Table 1.

The fifth and sixth properties listed above would be expected for Alfvén and/or fast waves. The seventh property would be expected

if waves propagating outwardly along the field predominated. The two groups, mentioned in connection with the frequency dependence of the coherence, may be inward and outward-bound waves with somewhat different power spectra. In this case, the properties of this frequency dependence would indicate that the outward-bound waves were somewhat less predominant at the higher frequencies. The presence of two such groups, i.e., inward and outward-bound waves, would also account for the eighth property listed above.

We remarked above that fast waves and/or Alfvén waves would produce the measured power-density ratios. In Part 1, it was shown that Alfvén waves alone could not produce the observed variations because the variations along $\vec{B}_o$ were of about the same magnitudes as those in the transverse directions. Thus, it would appear that the field variations were produced primarily either by fast waves and Alfvén waves or by fast waves alone.

These results do not indicate whether Alfvén waves were definitely present. Further, they do not indicate whether slow waves were present, but undetected due to the presence of waves in one or both of the other modes. Since the fast and slow modes are coupled in the ideal case, and since the Alfvén mode is not likely to be strictly decoupled in the interplanetary medium, it is probable that all three types of waves were encountered.

It should be mentioned also that the magnetic field measurements suggest that qualitatively similar variations occur in the range of frequencies up to at least 500 cpd. These field measurements provided information in the frequency range 0 - 1000 cpd. The data indicate that the properties of the field variations in the range 50 - 500 cpd are the same as those in the range 1 - 50 cpd, except that the absolute power densities decrease with increasing frequency, reaching the noise level of the magnetometer at about 500 cpd.

The auto spectra of the field variables were described in Part 1. At frequencies near 500 cpd, the spectra, in general, showed a frequency dependence somewhat weaker than f^{-2}. Of course, a cutoff would be expected near the proton cyclotron frequency of 0.08 cps. For Alfvén waves, this cutoff could appear in our computed spectra at frequencies up to about 1 cps due to Doppler shifts (compare Equations 8 and 8a). There is some evidence from OGO-1 [Holzer, McLeod, and Smith, 1966] that a steepening of the spectra of the field variables to a dependence stronger than f^{-2} occurs near 0.2 cps.

There are several likely sources for waves in the interplanetary medium. It has been suggested that the sun's chromosphere and corona result from the convective motion in the granulation zone of the photosphere [Leighton, 1963]. Acoustic waves generated by this motion are believed to travel upward or outward, through the atmosphere, transporting sufficient energy to provide heating of the upper layers. There is evidence that the periods of these waves are about 6 minutes,

which is roughly the mean lifetime of the granulation pattern. The preferred spacing of the cells in the pattern is about 2000 km.

There is another pattern or convective flow in the sun which corresponds to the more recently detected supergranulation. The coarser supergranulation is physically similar to the finer granulation, but behaves independently. The mean lifetime of the supergranulation pattern is evidently about 10 hours. The preferred spacing of these larger cells is about 35,000 km.

Waves produced by these two patterns of convective motion may produce disturbances in the interplanetary medium. In this case, we might expect variations which would be modulated with periods of about 10 hours and less, with the shorter periods due to harmonics, and variations with periods of 6 minutes and less. The sun's rotation would, of course, complicate the frequency spectrum that would be observed at a fixed point. Thus, from the waves corresponding to the granulation pattern, one would expect components with periods of 17 minutes and shorter and from the waves corresponding to the supergranulation pattern, one would expect components with periods of 4 hours and shorter.

In a discussion of interplanetary dynamical processes, Parker, [1963] described several other likely sources for disturbances in the interplanetary medium. Interactions between streams of solar plasma traveling at different velocities will occur since the coronal temperature varies with time and position. Such interactions may produce

disturbances traveling in both directions from the boundaries between the streams. Further, several types of instabilities are predicted for the case in which the solar wind is composed of many streams in each of which the plasma is in a different state.

In addition, the solar-wind model of Parker [1958] for the coronal expansion requires that the outwardly flowing plasma expand anisotropically. In the absence of collisions in the plasma, this is expected to generate plasma instabilities that could result in wave-like phenomena.

Acknowledgments

I wish to express my appreciation to M. M. Neugebauer and C.W. Snyder for permission to use data from the Mariner-2 plasma probe; to L. Davis, Jr., C. P. Sonett, and E. J. Smith with whom I collaborated on the magnetometer experiment, and to E. A. Kraut who has been kind enough to discuss with me many aspects of this analysis. The work was supported by the National Aeronautics and Space Administration under research grant NsG 249.

References

Alfvén, H., Cosmical Electrodynamics, Clarendon Press, Oxford, 1950.

Coleman, P.J., Jr., Variations in the interplanetary magnetic field: Mariner 2, Part 1. Observed properties, Publication No. 501, Institute of Geophysics and Planetary Physics, University of California, Los Angeles, 1966.

Coleman, P.J., Jr., L. Davis, Jr., E.J. Smith, and D.E. Jones, Variations in the polarity distribution of the interplanetary magnetic field, J. Geophys. Res., 71, (11), 2831-2839, 1966.

Holzer, R.E., M.G. McLeod, and E.J. Smith, Preliminary results from the Ogo 1 search coil magnetometer: Boundary positions and magnetic noise spectra, J. Geophys. Res., 71, (5), 1481-1486, March 1, 1966.

Leighton, R.B., The solar granulation, Annual Review of Astronomy and Astrophysics, 1, 19-40, 1963.

Neugebauer, M.M., and C.W. Snyder, The mission of Mariner II: Preliminary observations, solar plasma experiment, Science, 138, No. 3545, 1-2, December 7, 1962.

Neugebauer, M.M., and C.W. Snyder, Mariner-2 observations of the solar wind, Part 1. Average properties, Preprint, Jet Propulsion Laboratory, Pasadena, California, April, 1966.

Parker, E.N., Dynamics of the interplanetary gas and magnetic fields, Astrophys. J., 128, 664-676, 1958.

Parker, E.N., Interplanetary Dynamical Processes, 151-160, Interscience Publishers, New York, 1963.

Thompson, W.B., An Introduction to Plasma Physics, Chapter 5, Pergamon Press, New York, 1962.

Table Captions

Table 1. Results of calculations of power-density ratios, coherences squared, and phase differences for idealized hydromagnetic waves. In these calculations, $B_o = 5 \cdot 10^{-5}$ gauss, n = 5 protons/cm^3, T = 10^{5o}K. The phase difference, Φ, between a pair of variables is given by the sign of R, the square of the coherence, for the pair. Thus, the pair is in phase for $R > 0$ and 180^o out of phase for $R < 0$. Where two signs are given, the upper sign corresponds to the case of $\beta = 25^o$ and the lower sign is for $\beta = -25^o$. The quantity P for a particular variable is just the average power that would appear in a record of the variable that was one period of oscillation in length. In these calculations, it was assumed that the variations would be produced by a superposition of randomly polarized waves. For transverse waves the range of θ_k indicated by 'all' is $0 \leq \theta_k \leq 90^o$. The results given here are for the case $\vec{k} \cdot \vec{B}_o > 0$. For $\vec{k} \cdot \vec{B}_o < 0$, all phase differences change by 180^o.

Table 2. Ratios of the power densities, coherences squared, and phase differences obtained from six sets of auto and cross spectra for the measured variables B_r, B_θ, B_φ, and V_r. The power densities, P, the coherences squared, R, and the phase differences, Φ, are averages taken over the frequency range 1-50 cycles per day. The quantity R_{min} is the value of R required for a significant measurement of Φ, i.e., for a measurement in which the rms uncertainty of Φ is 45^o. A (+) polarity is assigned if the average field was directed outward from the sun; a (-) polarity is assigned if it was inward toward the sun.

Table 1

θ_k	θ_v	v_{ox}	$v_{o_\perp}$	θ_b	b_{ox}	$b_{o_\perp}$
Deg.	Deg.	v_o cm/sec		Deg.	$v_o \cdot 10^{-11}$ gauss	
Slow Mode						
0	0.0	1.00	0.00	-----	0.00	0.00
15	-15.0	0.97	0.26	103.5	0.10	0.36
30	-17.5	0.95	0.30	120.0	0.26	0.45
45	-15.0	0.97	0.26	135.0	0.41	0.41
60	-10.4	0.98	0.18	150.0	0.52	0.30
75	- 5.9	0.99	0.10	165.0	0.60	0.16
90	0.0	1.00	0.00	-----	----	----
Fast Mode						
0	90.0	0.00	1.00	-90.0	0.00	1.00
15	75.0	0.26	0.97	-74.8	0.25	0.92
30	72.5	0.30	0.95	-60.0	0.44	0.76
45	75.0	0.26	0.97	-45.0	0.60	0.60
60	79.6	0.18	0.98	-29.6	0.72	0.41
75	84.3	0.10	0.99	-15.0	0.79	0.21
90	90.0	0.00	1.00	0.0	0.82	0.00
Transverse Mode						
All	90.0	0.00	1.00	-90.0	0.00	1.00

Table 1 (cont'd)

θ_k	$P(B_r)/P(V_r)$	$P(B_\theta)/P(V_r)$	$P(B_\varphi)/P(V_r)$	$R(V_r, B_r)$	$\Phi(V_r, B_r)$
Deg.	10^{-23} gauss^2 cm^{-2} sec^2				Deg.
Slow Mode, $\beta = 0^\circ$					
0	0.00	0.00	0.00	0.00	---
15	0.58	1.17	0.76	-0.55	180°
30	1.48	1.83	1.58	-0.82	180°
45	2.35	1.48	2.10	-0.93	180°
60	3.12	0.79	2.43	-0.98	180°
75	3.65	0.22	2.64	-0.99	180°
90	3.84	0.00	2.71	-1.00	180°
Slow Mode, $\beta = \pm 25^\circ$					
0	0.00	0.00	0.00	0.00	---
15	0.83	1.19	1.00	-0.52	180°
30	1.84	2.06	1.95	-0.78	180°
45	2.64	2.10	2.39	-0.91	180°
60	3.28	1.82	2.59	-0.97	180°
75	3.70	1.54	2.68	-0.99	180°
90	3.84	1.42	2.71	-1.00	180°
Fast Mode, $\beta = 0^\circ$					
0	10.50	25.40	14.90	-1.00	180°
15	9.08	18.30	11.80	-0.66	180°
30	9.74	12.10	10.40	-0.30	180°
45	12.20	7.71	10.90	-0.11	180°
60	15.30	3.90	12.00	-0.02	180°
75	17.90	1.07	12.90	0.00	---
90	18.90	0.00	13.30	0.00	---
Fast Mode, $\beta = \pm 25^\circ$					
0	10.50	16.60	13.40	-1.00	180°
15	9.08	13.10	11.00	-0.76	180°
30	8.78	9.84	9.28	-0.48	180°
45	9.69	7.70	8.75	-0.28	180°
60	10.90	6.08	8.66	-0.15	180°
75	12.00	4.98	8.69	-0.06	180°
90	12.40	4.59	8.71	0.00	---
Transverse Mode, $\beta = 0^\circ$					
All	10.00	25.00	15.10	-1.00	180°
Transverse Mode, $\beta = \pm 25^\circ$					
All	7.70	16.00	10.80	-1.00	180°

Table 2

Period Days	Polarity	$P(B_r)/P(V_r)$	$P(B_\theta)/P(V_r)$	$P(B_\varphi)/P(V_r)$	$R(V_r, B_r)$	R_{min}	$\phi(V_r, B_r)$
		10^{-23} gauss^2 cm^{-2} sec^2					Deg.
243-252	+	11.8	16.5	14.5	.223	.021	181 ± 7
254-263	-	7.8	21.2	13.4	.050	.023	- 4 ±14
270-279	+	2.3	5.3	4.2	.039	.019	172 ± 8
282-291	-	14.4	31.7	29.3	.378	.023	4 ± 4
297-303	+	6.6	16.4	14.6	.487	.029	179 ± 4
313-318	-	46.1	32.3	32.3	.097	.035	6 ± 8
Average	+	6.9	12.7	11.1	.250		177
Average	-	22.8	28.4	25.0	.175		2
Average	Both	14.5	20.6	18.1	.213		

Figure Captions

Figure 1a. Spherical polar coordinate system with coordinates r, θ, and ϕ. Orthogonal unit vectors $\hat{r}$, $\hat{\theta}$, and $\hat{\phi}$ are shown at the point P, the location of the spacecraft. For simplification, the special case for the point $P(r, \theta = 0^{\circ}, \phi)$ is shown along with the magnetic line of force for the ideal spiral field [Parker, 1958] in the solar equatorial plane and passing through P.

Figure 1b. Orientation of the x y z axes relative to the r θ ϕ directions at point P for the special case in which $\vec{B}_o$ is in the rϕ plane.

Figure 1c. Orientation of the x y z axes relative to the r θ ϕ directions at a point P for the general case.

Figure 2. Orientation of an arbitrary vector $\vec{a}$ in the x y z system.

Figure 3. Ratios of power densities. The ratios of the power density in the auto spectrum of each vector field component to the power density in the auto spectrum of the radial component of the plasma velocity is plotted versus frequency for six sets of auto spectra. The theoretically allowed ranges for each ratio are also indicated on the right-hand side of the corresponding plot. Separate ranges are shown for each mode of propagation, fast (F), slow (S), and Alfvén or transverse (T).

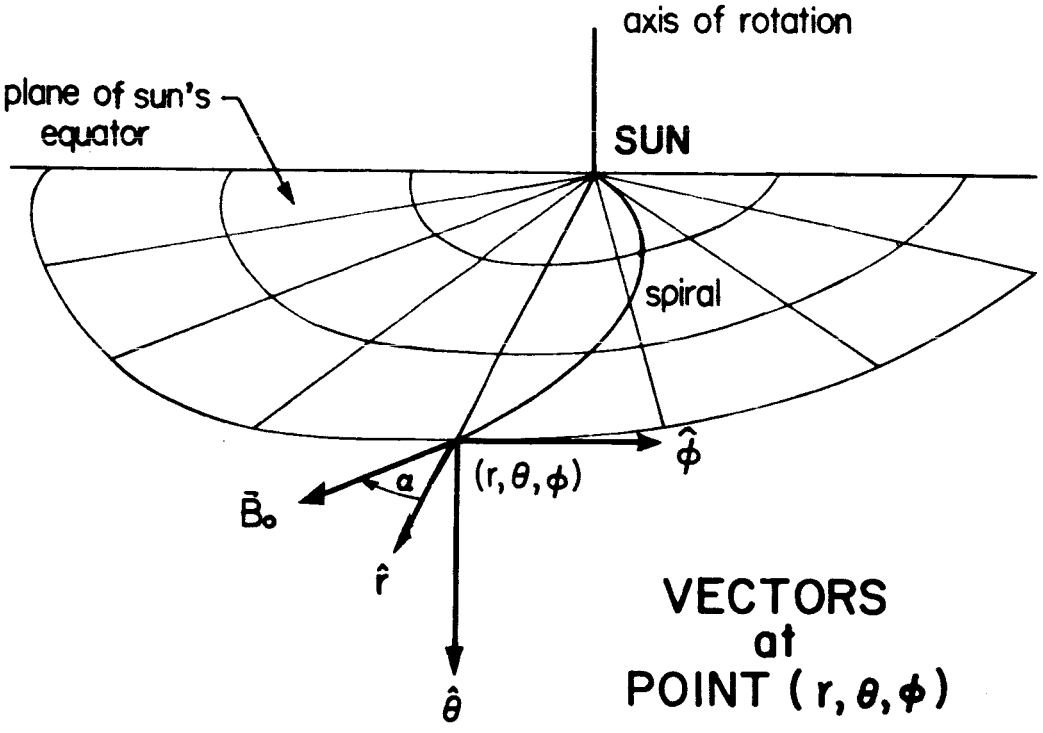

VECTORS at POINT (r, θ, ϕ)

(position of spacecraft)
special case, $\theta = 90°$
$\beta = 0°$

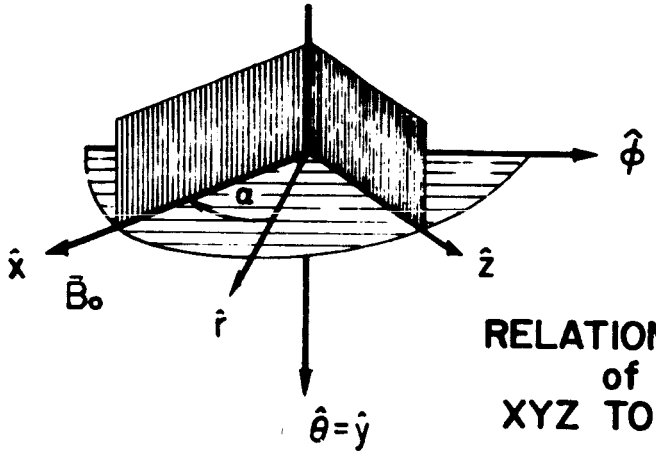

RELATIONSHIP of XYZ TO r $\theta\phi$

(special case)
$\beta = 0°$

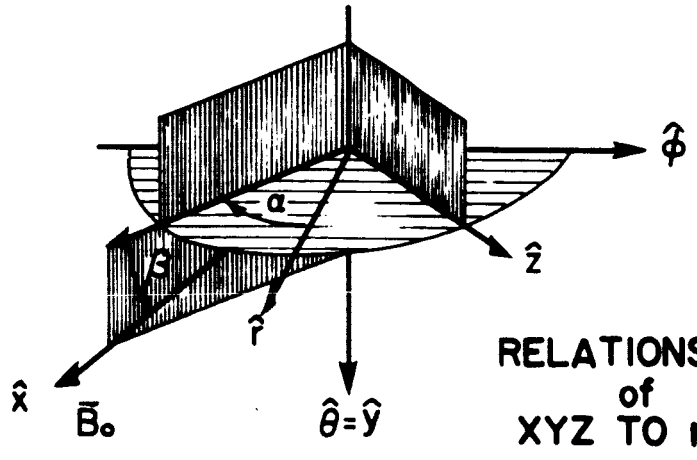

RELATIONSHIP of XYZ TO r $\theta\phi$

(general case)

Figure 1

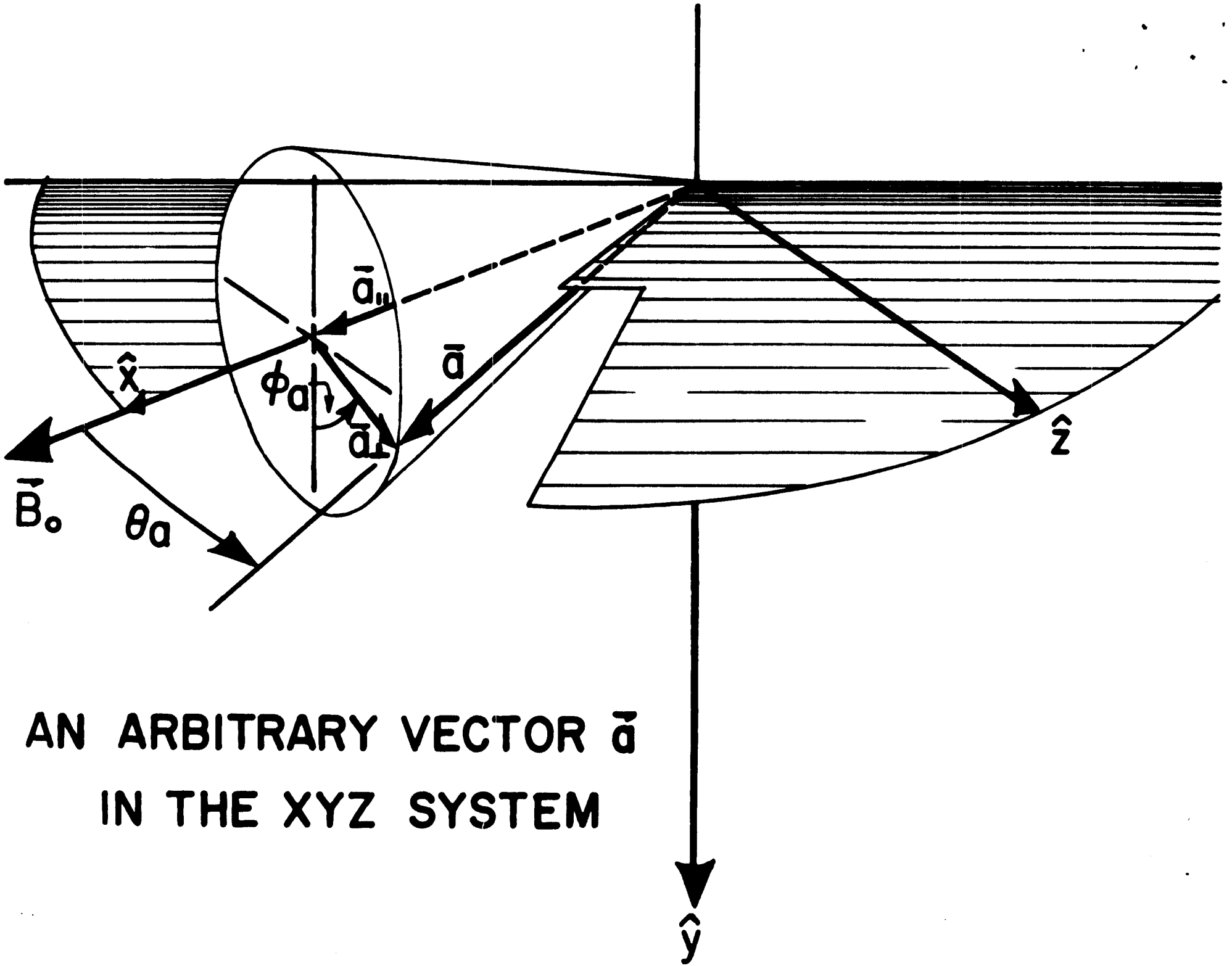
$\bar{a}_{\parallel}$
$\bar{a}$
$\hat{x}$
ϕ_a
$\bar{a}_{\perp}$
$\hat{z}$
$\bar{B}_o$
θ_a
$\hat{y}$
AN ARBITRARY VECTOR $\bar{a}$
IN THE XYZ SYSTEM

Figure 2

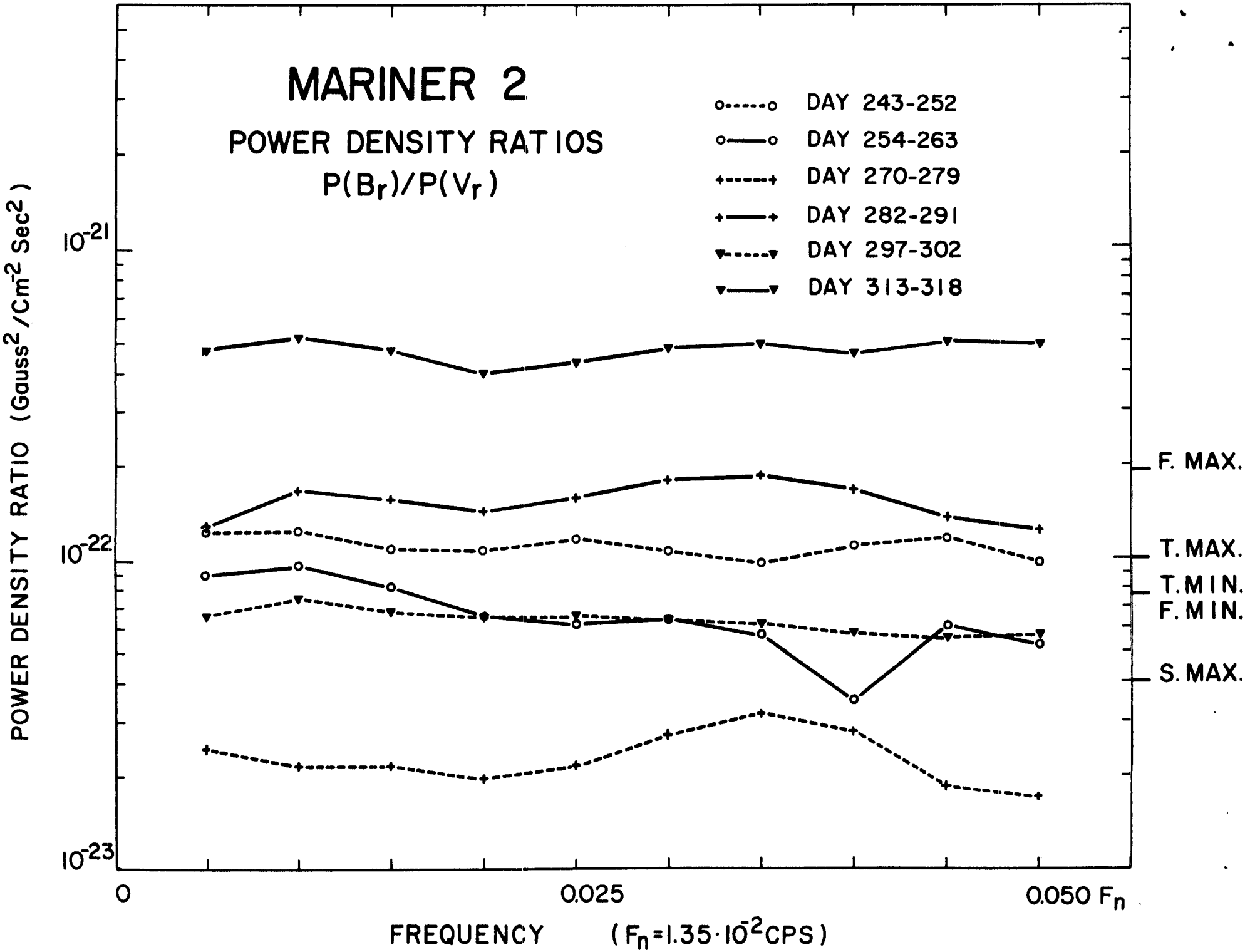
MARINER 2
POWER DENSITY RATIOS
P(Br)/P(Vr)
DAY 243-252
DAY 254-263
DAY 270-279
DAY 282-291
DAY 297-302
DAY 313-318
POWER DENSITY RATIO (Gauss²/Cm² Sec²)
10⁻²¹
10⁻²²
10⁻²³
F. MAX.
T. MAX.
T. MIN.
F. MIN.
S. MAX.
0
0.025
0.050 Fn
FREQUENCY (Fn=1.35·10⁻²CPS)

Figure 3a

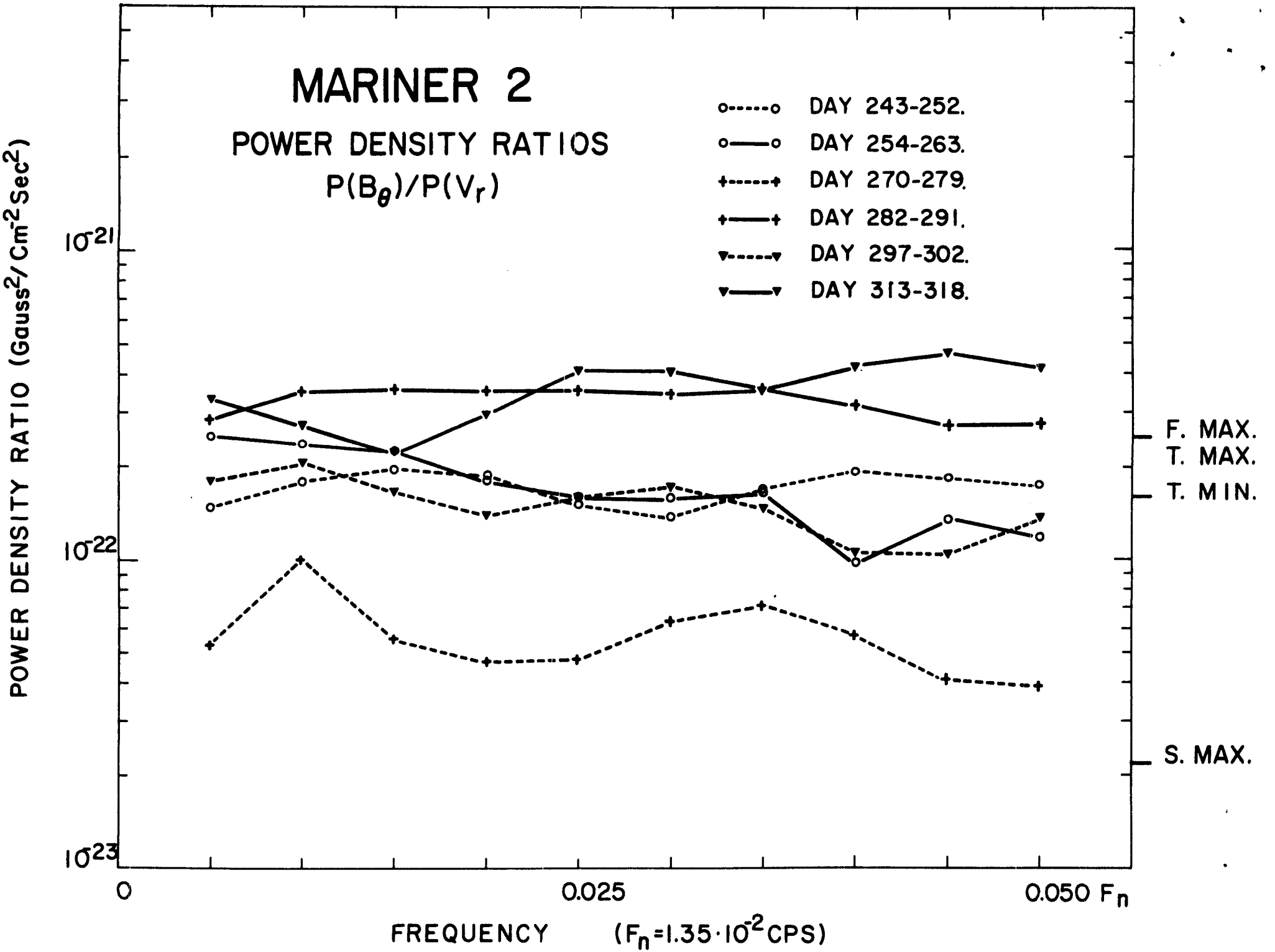
MARINER 2
POWER DENSITY RATIOS
$P(B_\theta)/P(V_r)$
DAY 243-252.
DAY 254-263.
DAY 270-279.
DAY 282-291.
DAY 297-302.
DAY 313-318.
POWER DENSITY RATIO (Gauss^2/Cm^{-2}Sec^2)
10^{-21}
10^{-22}
10^{-23}
F. MAX.
T. MAX.
T. MIN.
S. MAX.
0
0.025
0.050 F_n
FREQUENCY (F_n=1.35·10^{-2}CPS)

Figure 3b

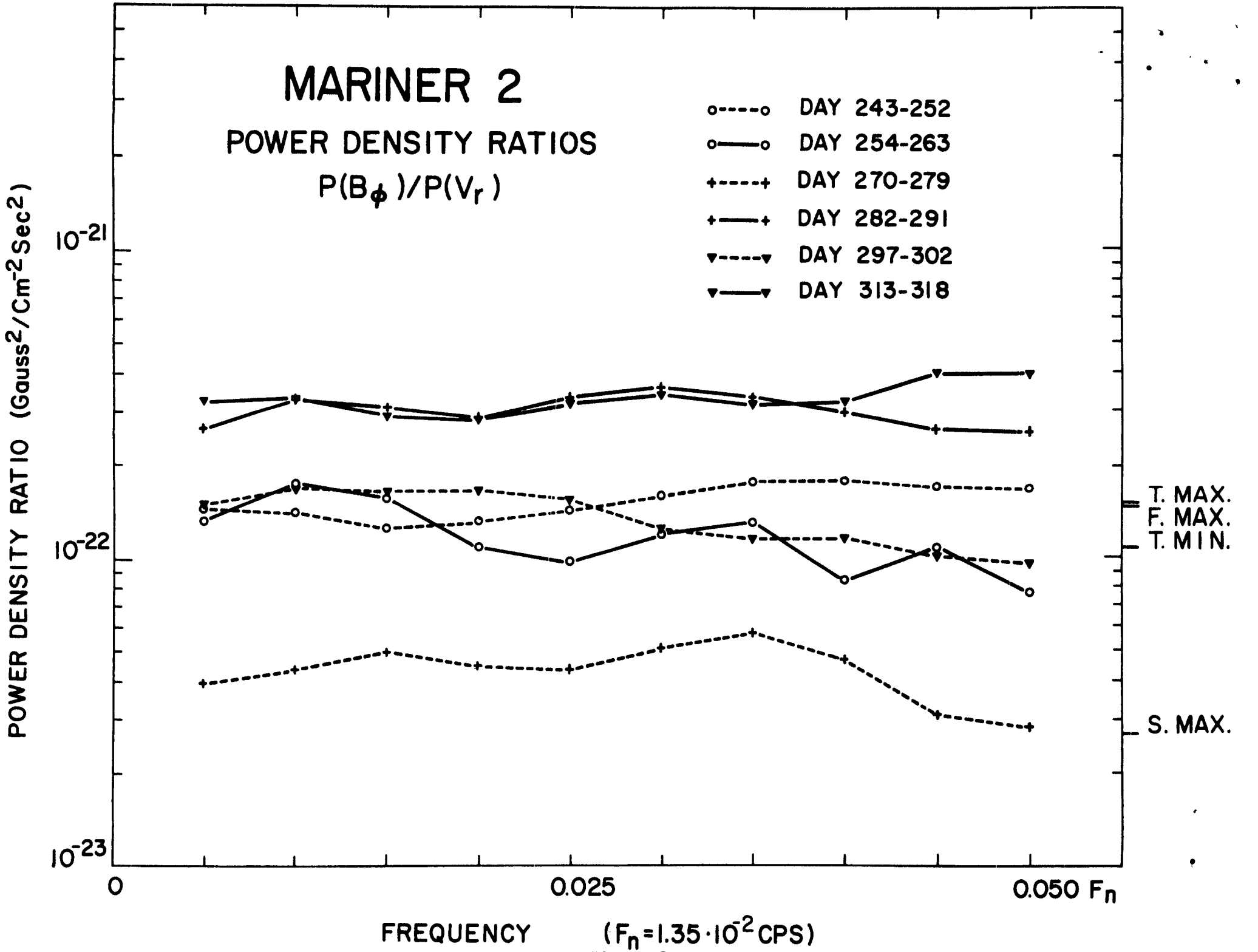
MARINER 2
POWER DENSITY RATIOS
$P(B_\phi)/P(V_r)$
DAY 243-252
DAY 254-263
DAY 270-279
DAY 282-291
DAY 297-302
DAY 313-318
POWER DENSITY RATIO (Gauss^2/Cm^{-2}Sec^2)
10^{-21}
10^{-22}
10^{-23}
T. MAX.
F. MAX.
T. MIN.
S. MAX.
0
0.025
0.050 Fn
FREQUENCY ($F_n = 1.35 \cdot 10^{-2}$ CPS)

Figure 3c